Targeting Curcusomes to Inflammatory Dendritic Cells Inhibits NF-κB and Improves Insulin Resistance in Obese Mice

Suman Kumar Yekollu, Ranjeny Thomas, and Brendan O'Sullivan

OBJECTIVE—To determine whether and by what mechanism systemic delivery of curcumin-containing liposomes improves insulin resistance in the leptin deficient (*ob/ob*) mouse model of insulin resistance.

RESEARCH DESIGN AND METHODS—Insulin resistant *ob/ob* mice with steatosis were injected intraperitoneally with liposome nanoparticles, entrapping the nuclear factor-κB (NF-κB) inhibitor curcumin (curcusomes), and uptake in liver and adipose tissue was determined by flow cytometry. The effects of curcusomes on macrophage NF-κB activation and cytokine production were assessed. Transfer experiments determined the role of hepatic tumor necrosis factor (TNF)/inducible nitric oxide synthase-producing dendritic cells (Tip-DCs) and adipose tissue macrophages (ATMs) in inflammation-induced insulin resistance, determined by homeostatic assessment of insulin resistance.

RESULTS—Phagocytic myeloid cells infiltrating the liver in *ob/ob* mice had the phenotypic characteristics of Tip-DCs that arise from monocyte precursors in the liver and spleen after infection. Targeting Tip-DCs and ATMs with curcusomes in *ob/ob* mice reduced NF-κB/RelA DNA binding activity, reduced TNF, and enhanced interleukin-4 production. Curcusomes improved peripheral insulin resistance.

CONCLUSIONS—Both hepatic Tip-DCs and ATMs contribute to insulin resistance in *ob/ob* mice. Curcusome nanoparticles inhibit proinflammatory pathways in hepatic Tip-DCs and ATMs and reverse insulin resistance. Targeting inflammatory DCs is a novel approach for type 2 diabetes treatment. ***Diabetes*** **60:2928–2938, 2011**

Patients with type 2 diabetes produce insulin, but insulin signaling of cells and, hence, glucose disposal is attenuated, leading to insulin resistance. In obesity, metabolic tissue promotes the infiltration and activation of macrophages that have a proinflammatory phenotype. In contrast, macrophages present in lean tissue are phagocytic and function in tissue remodeling (1). Nuclear factor-κB (NF-κB) is an important pathway in activation of this proinflammatory state, and ablation of this signaling pathway in myeloid cells in mice prevents diet- and genetic-induced insulin resistance (2). Studies on obese mice indicate that where calories are restricted after development of insulin resistance, macrophages switch to a less activated or alternate activated state (3). These findings confirm that the activation state of metabolic tissue-infiltrating macrophages is plastic and amenable to modulation.

The most promising treatments for type 2 diabetes are drugs that not only improve insulin signaling but also promote alternate macrophage activation, for example, thiazolidinediones, which are agonists of fatty acid sensors (4). However, these and other drugs do not cure type 2 diabetes, have unwanted side effects, and over time, patients may require increasing doses of insulin to regulate increasing blood glucose levels (5). Developing new drugs or approaches to promote alternate activation of macrophages represents a promising approach to treating diabetes.

Studies on genetically obese *ob/ob* mice and obese mice consuming a high-fat diet have shown that oral curcumin inhibits macrophage infiltration of adipose tissue and NF-κB activation in the liver; increases the production of the adipokine adiponectin in adipose tissue; and ameliorates inflammation, hyperglycemia, and insulin resistance (6). Although pharmacologically safe, curcumin has poor bioavailability after oral administration (7). Liposomal delivery systems have been used to enhance the bioavailability and improve the delivery of curcumin (8). As a result of the high hydrophobicity of curcumin, these curcumin-containing liposomes (curcusomes) are stable when diluted and incubated in vitro or injected in vivo (9,10). We have shown that curcusomes are taken up by splenic and lymph node antigen-presenting cells, including macrophages, dendritic cells (DCs), and B cells in vivo; block NF-κB activity in these cells; and inhibit inflammatory disease in mouse models of antigen-induced arthritis (10).

Given the capacity of curcusomes to target and block inflammatory activity of phagocytic antigen-presenting cells, we tested their effects in the *ob/ob* mouse model of obesity and hepatic and peripheral insulin resistance. The data indicate that tumor necrosis factor/inducible nitric oxide synthase (TNF/iNOS)-producing DCs (Tip-DCs) in *ob/ob* livers are inhibited and modulated by curcusomes, resulting in improvements in peripheral insulin resistance.

RESEARCH DESIGN AND METHODS

Leptin deficient (C57BL/6J, *ob/ob*) mice and nonobese control mice were bred in-house under pathogen-free conditions.

Analysis of liver cell populations. Whole liver was harvested from mice and digested with Collagenase Type III (Worthington, Lakewood, NJ) for 30 min at 37°C, and leukocytes were purified by density gradient centrifugation with 30% Histodenz (Sigma Aldrich, Castle Hill, NSW). Leukocytes were stained with antibodies to detect macrophages (MHC II+, CD11b+, and F4/80+), natural killer T (NKT) cells (CD3+ and NK1.1+), T cells (CD4+ and CD8+), plasmacytoid DCs (pDCA1+), and B cells (CD19+). Cell proportions were determined by flow cytometry. Inflammatory macrophages were purified using CD11c+ bead enrichment (Miltenyi, North Ryde, NSW); cultured in media for 24 h in the presence of lipopolysaccharide (LPS), recombinant γ-interferon (IFN-γ), and brefeldin;

From the University of Queensland Diamantina Institute, Woolloongabba, Queensland, Australia.
Corresponding author: Brendan O'Sullivan, uqbosull@uq.edu.au.
Received 27 February 2011 and accepted 19 July 2011.
DOI: 10.2337/db11-0275
This article contains Supplementary Data online at http://diabetes.diabetesjournals.org/lookup/suppl/doi:10.2337/db11-0275/-/DC1.

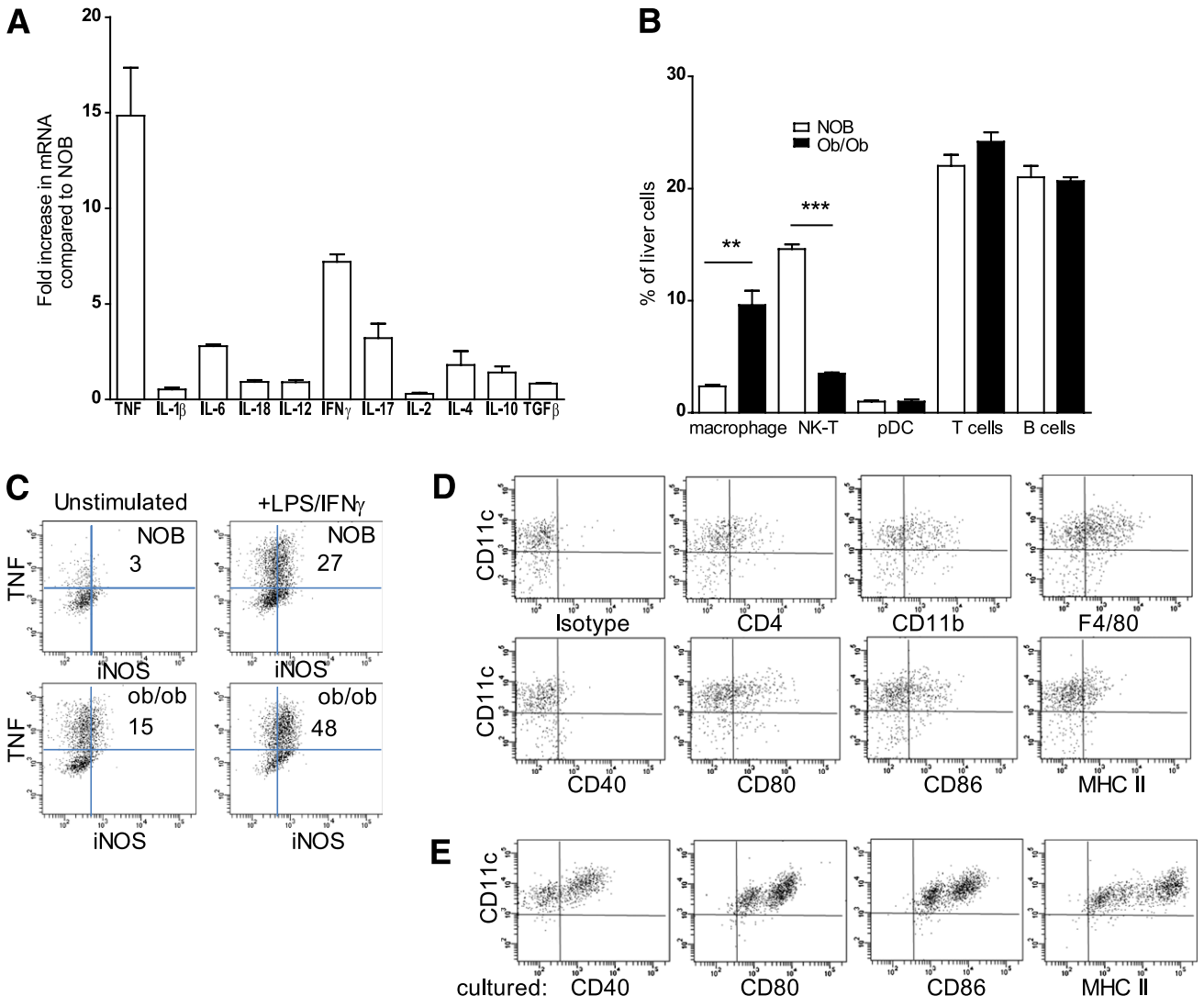

FIG. 1. Inflammatory liver DCs in *ob/ob* mice. *A*: Hepatic mRNA was purified from 12-week-old *ob/ob* mice or 12-week-old nonobese littermate controls (NOB) and analyzed by qPCR for relative expression of cytokines. Shown is the fold increase in cytokine expression comparing RNA from *ob/ob* liver with NOB liver. Data are mean ± SEM of two separate experiments analyzing individual mice. *B*: Gradient-purified cells isolated from the livers of 12-week-old *ob/ob* mice or NOB mice were stained for surface markers against leukocyte subsets and analyzed by flow cytometry. **$P \leq 0.01$, ***$P \leq 0.001$ (one-way ANOVA followed by Bonferroni post hoc test). Data are mean ± SEM of two separate experiments analyzing individual mice. pDC, plasmacytoid DC. *C*: CD11c+ cells were purified by magnetic bead selection from gradient-enriched liver leukocytes from 12-week-old *ob/ob* mice or NOB mice. Cells were cultured with or without LPS for 24 h in the presence of brefeldin and then stained for intracellular TNF and iNOS. Shown are flow cytometry analysis of cells and percentage of cells staining positive for TNF and iNOS. Data are mean ± SEM of two separate

permeabilized; and then stained for intracellular expression of TNF (Biolegend, San Diego, CA) and iNOS (NOS2, M-19, Santa Cruz, Santa Cruz, CA). Inflammatory macrophages were cultured for 48 h in the presence or absence of LPS; stained for CD40, CD80, CD86, and MHC class II (Biolegend); and analyzed by flow cytometry.

Liposome formulations. Curcumin (1,7-bis[4-hydroxy-3-methoxyphenyl]-1,6-heptadiene-3,5-dione) (a high lipophilicity; log $P > 3$) and the fluorescent marker DiI (Invitrogen Molecular Probes, Mulgrave, Victoria, Australia) were encapsulated into liposomal formulations under sterile conditions as previously described (10).

Analysis of peritoneal macrophages. Peritoneal macrophages were harvested from *ob/ob* mice by peritoneal lavage. Cells were cultured with curcusomes or free curcumin in the presence or absence of LPS. Interleukin (IL)-6 was measured in supernatants 6 h later by cytokine bead array (BD Bioscience, San Jose, CA). Peritoneal macrophages were harvested from *ob/ob* mice 24 h after injection with curcusomes or empty liposomes, and cells were cultured for 1, 6, and 24 h in media with or without LPS. At 1 h, nuclear extracts were prepared and cells analyzed for nuclear RelA DNA binding by enzyme-linked immunosorbent assay (ELISA). At 6 h, supernatants were harvested and IL-6 levels measured by intracellular cytokine staining. At 24 h, cytospins of cells were prepared and cells fixed in 4% paraformaldehyde and stained with CD11c-Alexa-655, p50 or RelA (two-step staining with anti-rabbit Alexa-555), and DAPI.

Analysis of adipose tissue macrophages. To isolate stromal vesicular fractions, gonadal fat was excised from mice and digested with Collagenase Type III (Worthington) for 30 min at 37°C. Digested tissue was passed through a cell strainer and then centrifuged at 500*g* for 5 min before removing erythrocytes by incubation in ammonium chloride solution. Cells were analyzed for DiI uptake by staining with antibodies for MHC II+ and F4/80+ cells and then measuring DiI levels by flow cytometry. CD11c+ macrophages were purified from stromal vesicular fractions cells isolated from *ob/ob* mice treated with or without curcusomes for 24 and 72 h and analyzed for cytokine gene expression by quantitative real-time PCR (qPCR). CD11c+ macrophages were also cultured with and without LPS for 1 h, and nuclear extracts were prepared and RelA levels determined by DNA binding ELISA.

Metabolic studies. A one-touch glucose monitoring system was used to obtain glucose measurements from blood isolated from mice fasted 6 h. Insulin (Crystal Chem Inc., Downers Grove, IL) and adiponectin levels (Biovision, Mountain View, CA) were measured by ELISA using serum from fasted mice. For glucose tolerance tests (GTTs), fasted mice were injected intraperitoneally with glucose (1 g/kg), and blood samples were taken at 15, 30, 60, and 120 min for glucose measurements. Homeostasis model assessment of insulin resistance (HOMA-IR) was calculated using fasting glucose and insulin measurements and the HOMA calculator (Diabetes Trials Unit, University of Oxford, Oxford, U.K.). A total of 1×10^6 F4/80+ Tip-DCs or ATMs isolated from *ob/ob* mice, either injected 72 h previously with curcusomes or empty liposomes, were purified by magnetic bead enrichment and injected intravenously into 8-week-old C57BL/6J mice. After 72 h, GTTs were performed on fasted mice.

Measurement of oxidative burst. Levels of reactive oxygen species released from peritoneal macrophages were measured using the luminol-enhanced chemiluminescence assay as previously described (11). A total of 10^5 macrophages per well were stimulated with opsonized zymosan at 37°C for 45 min to induce an oxidative burst measured as relative light units.

NF-κB/RelA DNA binding ELISA. RelA DNA binding activity was measured by chemiluminescent ELISA as previously reported (12). Data are expressed as a ratio of signal to background with background measurements carrying out the assay in the absence of nuclear extracts.

Gene expression. Total RNA was isolated from liver or F4/80 purified macrophages with Trizol and reverse transcribed using a Superscript III kit (Invitrogen). qPCR was carried out using primers designed to amplify mouse cytokines and normalized to expression of hypoxanthine guanine phosphoribosyl transferase.

Preparation of tissue lysates and immunoblotting. Overnight-fasted mice were anesthetized and injected with 5 units of insulin into the portal vein and then killed 5 min postinjection. Liver and quadriceps were immediately isolated and snap frozen in dry ice and stored at −80°C. Tissues were homogenized using an Utra-Turrax T25 (IKA, Wilmington, NC) in T-Per Buffer (Pierce, Rockford, IL) containing protease inhibitors (Roche, West End, QLD, Australia). A total of 50 μg of protein was separated by SDS-PAGE and transferred to polyvinylidene fluoride membranes before immunoblotting with (ser473) or AKT (Cell Signaling, Danvers, MA).

Statistical analysis. One-way ANOVA analysis with Bonferroni multiple comparison posttest compared multiple means. Significance is indicated as $^*P < 0.05$, $^{**}P < 0.005$, and $^{***}P < 0.001$. All error bars represent SEM.

RESULTS

The liver of *ob/ob* mice is enriched in Tip-DCs. To determine the extent of inflammation in the livers of obese mice, we first examined proinflammatory cytokine expression by qPCR of RNA isolated from livers of 12-week-old *ob/ob* mice and age-matched *ob/wt* (NOB) livers. Expression of typical macrophage proinflammatory genes, including *TNF* (15-fold) and *IL-6* (3-fold), was increased in obese relative to NOB mice (Fig. 1*A*). The T-cell cytokines IFN-γ (5-fold) and IL-17 (3-fold) were also increased in obese livers. There were no differences in the percentages of CD3+ T cells, CD19+ B cells, and pDCA1+ plasmacytoid DCs when comparing *ob/ob* and NOB mice. However, consistent with liver inflammation, a reduction in the proportion of CD3+NK1.1 NKT cells and an increase in proportion of MHC class II+ CD11b+ F4/80+ macrophages was observed in livers from *ob/ob* mice compared with age-matched NOB mice (Fig. 1*B*). These cells also expressed CD11c, which is broadly expressed by murine DC populations. We used CD11c immunoselection to isolate and further characterize this cell population from the liver. In particular, given their inflammatory environment, we sought other markers of DCs described recently to develop from inflammatory monocytes in response to infection in the liver and spleen, known as Tip-DCs because of their expression of TNF and iNOS (13).

After isolation from the liver of *ob/ob* mice, the CD11c+ cells expressed higher levels of iNOS and TNF compared with NOB controls, without or with LPS and IFN-γ stimulation (Fig. 1*C*). The majority of CD11c+ cells purified from *ob/ob* mice livers expressed CD11b and F4/80, low levels of MHC class II and CD40, and intermediate CD80 and CD86 (Fig. 1*D*). After 48-h culture in medium, CD40, CD80, CD86, and MHC class II were upregulated (Fig. 1*E*). Activation with the toll-like receptor (TLR) agonist LPS had no additional effects on costimulatory molecule upregulation (data not shown).

To examine the distribution of CD11c+F4/80+ cells within *ob/ob* livers, immunofluorescent staining of liver sections from *ob/ob* mice was performed. Large fat bodies surrounded by F4/80+CD11c+ cells were observed in liver sections from the *ob/ob* mice but not from NOB mice, a characteristic pattern observed with liver steatosis (Fig. 1*F*). Consistent with the increased TNF mRNA expression, strong nuclear staining of p65/RelA was observed in CD11c+F480+ inflammatory macrophages surrounding fat deposits, whereas p65/RelA staining was predominantly cytoplasmic in liver sections from NOB mice (Fig. 1*F*).

These data indicate that the fatty liver of *ob/ob* mice is enriched in typical CD11c+ Tip-DCs, expressing costimulatory molecules, high levels of p65/RelA nuclear staining, and TNF/iNOS. This phenotype indicates their capacity to promote inflammation associated with fatty infiltration and insulin resistance and is a potential target for therapeutics that inhibit NF-κB.

experiments analyzing individual mice. *D*: CD11c purified liver cells from *ob/ob* mice were stained for surface markers, costimulatory molecules, and MHC class II and analyzed by flow cytometry. *E*: CD11c+ DCs purified from livers of *ob/ob* mice were cultured for 48 h, stained for costimulatory molecules and MHC class II, and analyzed by flow cytometry. *F*: Livers from 12-week-old *ob/ob* mice or NOB mice were harvested, frozen in optimal cutting temperature media, sectioned, and stained with RelA (red) and CD11c (blue) antibodies. Arrows indicate nuclear RelA in CD11c+ cells. Original magnification ×25. (A high-quality digital representation of this figure is available in the online issue.)

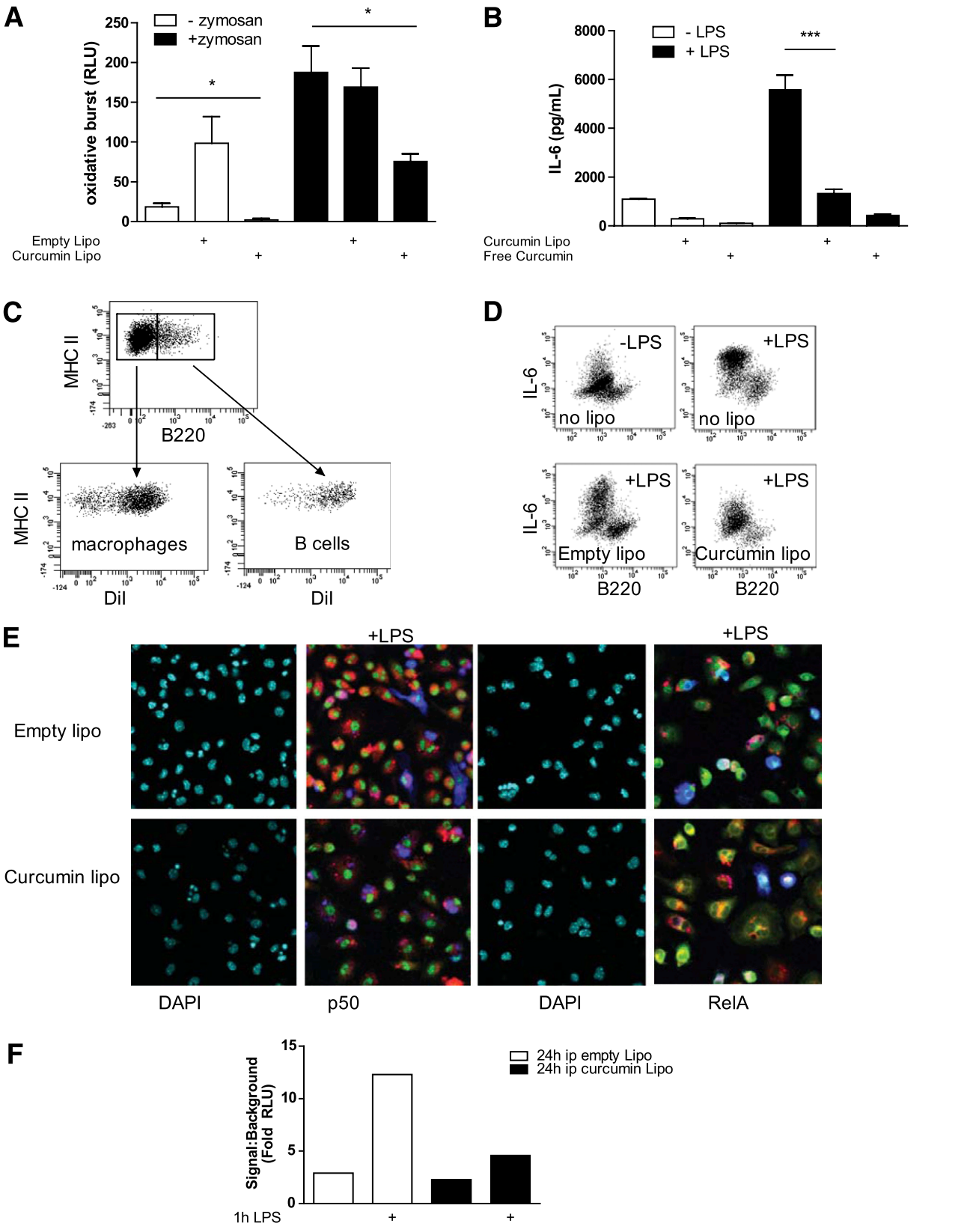

FIG. 2. Curcusomes inhibit oxidative burst, cytokine production, and NF-κB in peritoneal macrophages from *ob/ob* mice. *A*: Cells isolated from peritoneal exudates from *ob/ob* mice were cultured for 30 min with or without zymosan in the presence of 1 μg/mL final concentration of empty liposomes or curcusomes. Oxidative burst was measured by chemiluminescence and was expressed as relative light units (RLUs). *$P \leq 0.05$ (one-way ANOVA followed by Bonferroni post hoc test). Data are mean ± SEM of two separate experiments analyzing peritoneal exudates pooled from three mice. *B*: Cells isolated from peritoneal exudates from *ob/ob* mice were cultured in media for 6 h with or without LPS in the presence of 1 μg/mL final concentration of empty liposomes or curcusomes. Shown is IL-6 concentration in supernatants measured by cytokine bead array. ***$P \leq 0.001$ (one-way ANOVA followed by Bonferroni post hoc test). Data are mean ± SEM of two separate experiments analyzing peritoneal exudates pooled from three mice. *C*: *Ob/ob* mice were injected intraperitoneally with DiI-curcusomes, and 24 h later, cells from peritoneal exudates were harvested and

Curcusomes suppress NF-κB pathways and proinflammatory cytokine production in peritoneal macrophages. Curcusomes target and inhibit proinflammatory pathways of phagocytic antigen-presenting cells, including macrophages and DCs in healthy mice or mice with inflammatory arthritis (10). To test whether curcusomes inhibited inflammatory function of macrophages in the setting of obesity, peritoneal macrophages were isolated from *ob/ob* mice and cultured with either curcusomes or empty liposomes in the presence or absence of opsonized zymosan to induce an oxidative burst. In vitro, curcusomes—but not empty liposomes—inhibited the oxidative burst, indicating an antioxidant effect (Fig. 2*A*). Next, their effect on proinflammatory cytokine production was examined in macrophages cultured with LPS for 6 h in the presence or absence of curcusomes and free curcumin (Fig. 2*B*). Consistent with an anti-inflammatory effect, curcusomes or soluble curcumin inhibited LPS-induced IL-6 production in supernatants from macrophage cultures. These data indicate that curcusomes inhibit the oxidative burst and production of proinflammatory cytokines by macrophages in response to inflammatory triggers in vitro.

Next, in vivo uptake and effects of curcusomes on peritoneal macrophages were tested by injecting DiI-labeled curcusomes intraperitoneally into *ob/ob* mice. In the peritoneal cavity, curcusomes were taken up by macrophages and B cells (Fig. 2*C*). Stimulation with LPS indicated that F4/80+ macrophages were the main producers of IL-6, and this LPS-induced IL-6 could be inhibited by including curcumin in the liposome formulations (Fig. 2*D*). Curcusomes reduced the level of LPS-induced nuclear p65/RelA as assessed by immunofluorescence microscopy and p65/RelA DNA binding activity by ELISA (Fig. 2*E* and *F*). These data indicate that curcusomes target macrophages in vitro and in vivo and inhibit LPS-induced NF-κB and proinflammatory cytokine production.

Curcusome therapy suppresses NF-κB and proinflammatory cytokine production by Tip-DCs. To determine whether curcusomes also inhibited liver inflammatory Tip-DCs after intraperitoneal injection into *ob/ob* mice, we analyzed liver cells for uptake of DiI-curcusomes. Maximal curcusome uptake was observed at 72 h, where 30% of CD11c+F4/80+ cells were DiI+ (Fig. 3*A*). This was independent of liver steatosis, since NOB mice showed similar uptake of curcusomes. Immunofluorescent staining of liver sections from *ob/ob* mice injected with curcusomes 72 h earlier confirmed that Tip-DCs surrounding hepatocytes are the predominant cell type taking up liposomes (Fig. 3*B*).

Consistent with nuclear staining of Tip-DCs for p65/RelA, the constitutive p65/RelA DNA binding detected in nuclear extracts of Tip-DCs isolated from livers of *ob/ob* mice was further inducible after 1-h culture with LPS (Fig. 3*C*). In contrast to *ob/ob* mice, p65/RelA DNA binding in nuclear extracts from Tip-DCs isolated from livers of *ob/ob* mice treated with curcusomes was reduced and failed to increase in response to LPS signaling (Fig. 3*C*). To characterize the impact of curcusome delivery on Tip-DC function, we assessed cytokine expression in Tip-DCs by qPCR. Tip-DCs isolated from *ob/ob* mice expressed lower levels of IL-4 compared with untreated *ob/ob* mice (Fig. 3*D*). Moreover, curcusomes enhanced IL-4 mRNA expression by Tip-DCs, an effect not seen with empty liposomes. The other major impact of curcusome delivery was reduced expression of TNF and IL-6 mRNA compared with untreated *ob/ob* mice at 72 h (Fig. 3*E*). No changes in the proportion of CD11c+ DCs, CD11c+F480+ Tip-DCs, F480+ macrophages, plasmacytoid DCs, and NKT cells were observed 72 h after curcusome injection (Supplementary Fig. 1).

The data indicate that inflammatory Tip-DCs in the liver are targets in vivo of intraperitoneal injection of curcusomes. The result is a reduction in NF-κB DNA binding, enhanced IL-4, and reduced TNF and IL-6.

Curcusome therapy improves insulin resistance in *ob/ob* mice. Compared with NOB mice, *ob/ob* mice have increased fasting glucose and insulin, leading to a higher HOMA-IR (Fig. 4*A*–*C*). Treatment of *ob/ob* mice with curcusomes for 72 h reduced fasting glucose, insulin, and HOMA-IR to levels observed in NOB mice (Fig. 4*C*). GTTs confirmed that insulin resistance was improved after curcusome treatment, with a significant improvement in glucose uptake after glucose challenge (Fig. 4*D*). The improvement in HOMA-IR with curcusomes correlated with an increase in serum levels of the insulin-sensitizing adipokine adiponectin (Fig. 4*E*). The increase in adiponectin indicated that adipose tissue function was affected by curcusome delivery.

To determine if insulin sensitization was improved longer term after curcusome treatment, *ob/ob* mice were injected with a single dose of curcusomes and HOMA-IR assessed after 4 weeks. Compared with age-matched nontreated controls, *ob/ob* mice treated with curcusomes showed reduced HOMA-IR (Fig. 4*F*).

To assess tissue-specific effects on insulin signaling after curcusome treatment, fasted *ob/ob* mice, treated or untreated with curcusomes, were injected with insulin and pAKT levels were determined in the liver and skeletal tissue. Increased levels of insulin-induced pAKT were observed in the liver and skeletal muscle of *ob/ob* mice treated with curcusomes, indicating systemic improvements in insulin signaling after curcusome treatment (Fig. 5).

Given that curcusomes are widely taken up and inhibitory of inflammatory macrophages and DCs in *ob/ob* tissues, we also examined their uptake and effects on ATMs. We injected curcusomes and examined uptake by ATMs at 24 and 72 h by flow cytometry (Fig. 6*A*). Of ATMs, 35% were DiI+ and DiI uptake was maximal at 72 h, similar to the levels of uptake seen in the liver. Moreover, the cells that took up curcusomes were CD11b+F4/80+CD11c+ macrophages similar to liver Tip-DCs and were similarly located in "crown-like" structures surrounding large fat-laden adipocytes (Fig. 6*B*). Isolated adipose tissue inflammatory DCs demonstrated nuclear staining for p65/RelA and p50 but cytoplasmic staining for c-Rel, p52, and RelB, indicating activation of the classical but not alternate NF-κB pathway (Supplementary Fig. 2). Nuclear p65/RelA staining was

stained for MHC class II and B220. Shown is DiI uptake by both macrophages and B cells. Data representative of five separate experiments. *D*: Cells isolated from peritoneal exudates from *ob/ob* mice injected intraperitoneally with DiI-labeled empty liposomes or curcumin liposomes were cultured with or without LPS for 24 h in the presence of brefeldin and then stained for surface B220 and intracellular IL-6. Shown are flow cytometry plots with B220-negative macrophages as the main source of IL-6. Data representative of two separate experiments. *E*: Cells in *C* were adhered to chamber slides for 1 h in the presence of LPS and then stained for RelA (green) or p50 (green), CD11c (blue), and DAPI (cyan). DiI staining is shown in red; images acquired by immunofluorescence microscopy. Original magnification ×25. Data representative of three separate experiments. *F*: Nuclear extracts from cells in *C* were analyzed for DNA binding of RelA by chemiluminescence. Shown is the mean of duplicates from two separate experiments. Ip, intraperitoneally. (A high-quality digital representation of this figure is available in the online issue.)

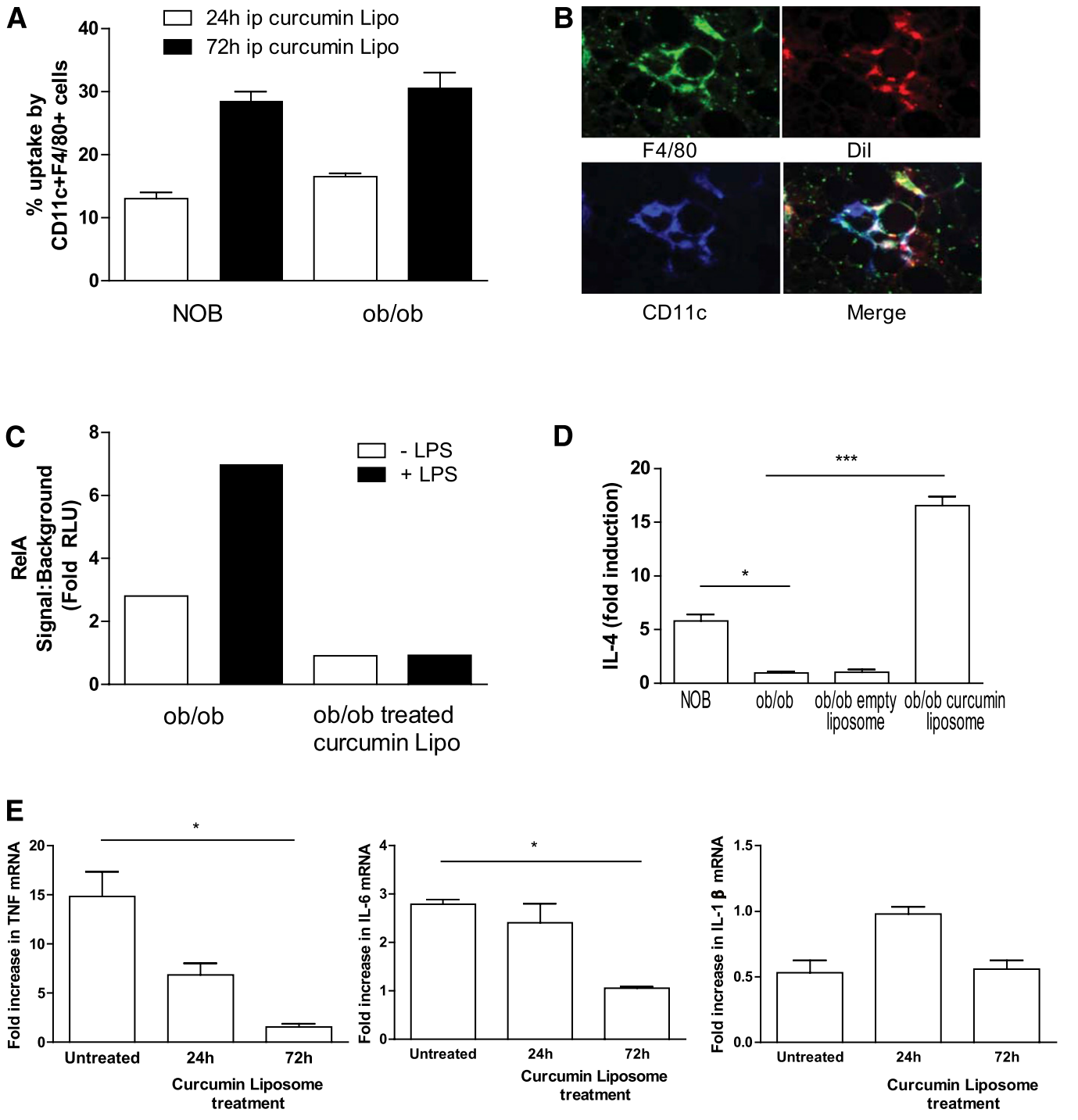

FIG. 3. In vivo delivery of curcusomes inhibits hepatic inflammatory DC cytokine production and nuclear RelA. *A*: *Ob/ob* and NOB mice were injected intraperitoneally (ip) with DiI-curcusomes, and gradient-purified liver cells were harvested at 24 and 72 h and stained for MHC class II, CD11c, and F4/80. Shown are the percentages of CD11c+ F4/80+ cells that are DiI+. Data are mean ± SEM of two separate experiments. *B*: *Ob/ob* mice were injected intraperitoneally with DiI-curcusomes for 72 h and then livers were harvested, frozen in optimal cutting temperature media, sectioned, and stained with F4/80 (green) and CD11c (blue) antibodies. DiI staining is indicated in red; images analyzed by immunofluorescence microscopy. Original magnification ×25. *C*: Nuclear extracts from CD11c+ liver cells isolated from *ob/ob* mice treated with or without curcusomes and cultured for 1 h with or without LPS were analyzed for DNA binding of RelA by chemiluminescent ELISA. Shown is the mean of duplicates from two separate experiments. *D*: mRNA from CD11c+ liver cells isolated from NOB mice and *ob/ob* mice treated with or without curcusomes for 72 h were analyzed by qPCR for relative expression of IL-4. *E*: mRNA from CD11c+ liver cells isolated from *ob/ob* mice treated with or without curcusomes for 24 and 72 h were analyzed by qPCR for relative expression of TNF, IL-6, and IL-1β. Shown is the fold increase in cytokine expression relative to the lowest expressing sample. Data are mean ± SEM of two separate experiments analyzing individual mice. *$P \leq 0.05$, ***$P \leq 0.001$ (one-way ANOVA followed by Bonferroni post hoc test). (A high-quality digital representation of this figure is available in the online issue.)

reduced in ATMs isolated from adipose tissue of *ob/ob* mice treated with curcusomes for 72 h (Fig. 6*C*).

Since both hepatic Tip-DCs and inflammatory ATMs are targeted by curcusomes, we determined which cell type promotes insulin resistance by isolating hepatic Tip-DCs and ATMs from *ob/ob* mice and adoptively transferring each population to NOB mice. At 72 h later, we analyzed the metabolic effect with a GTT in fasting

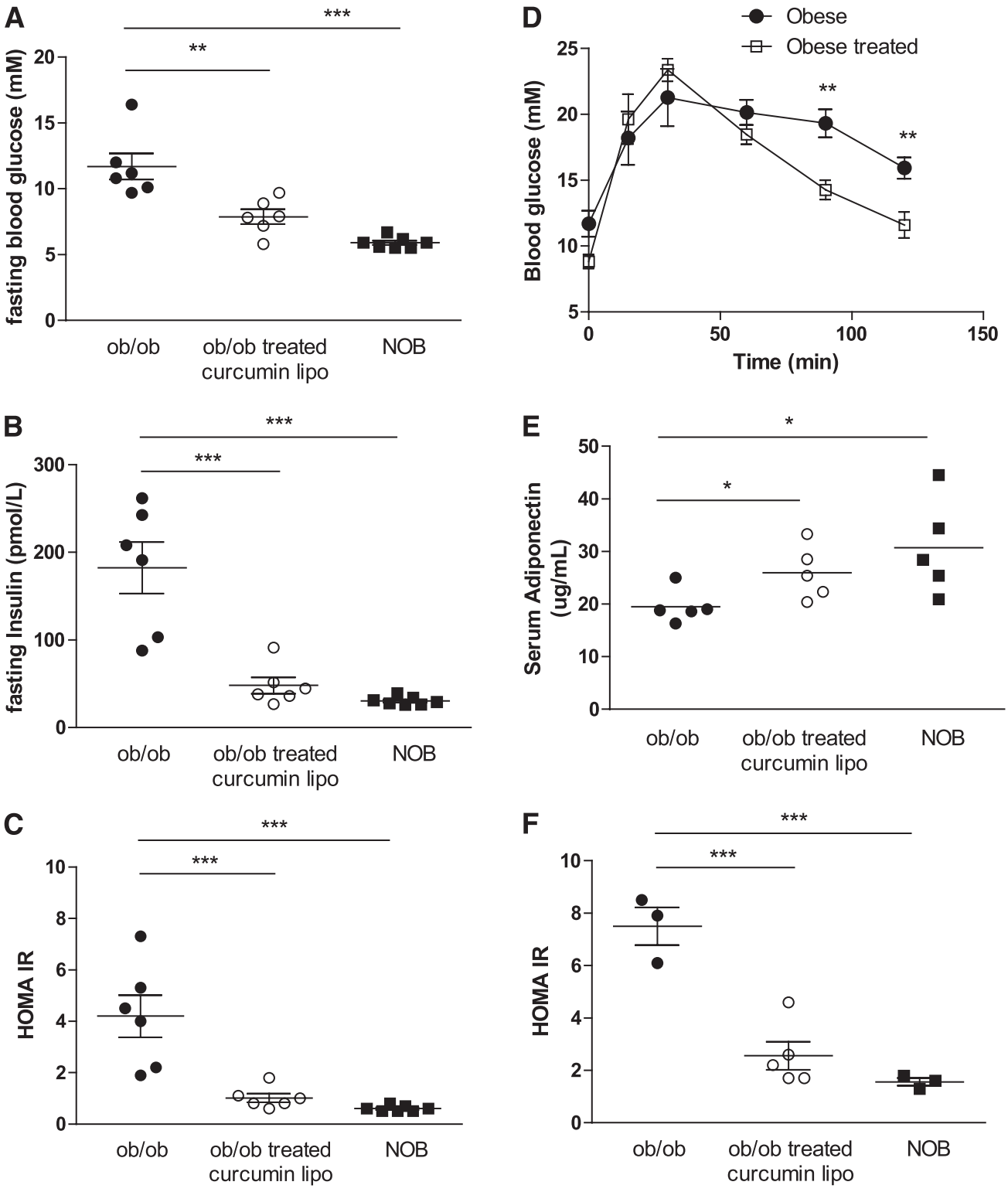

FIG. 4. Improved insulin signaling in *ob/ob* mice treated with curcusomes. Fasting blood glucose (*A*), insulin (*B*), and HOMA-IR (*C*) from *ob/ob* mice injected intraperitoneally with curcusomes for 72 h. ***$P \leq 0.001$, **$P \leq 0.01$ (one-way ANOVA followed by Bonferroni post hoc test). *D*: GTT from mice treated in *A*. **$P \leq 0.01$ (one-way ANOVA followed by Bonferroni post hoc test). *E*: Serum adiponectin levels from mice treated in *A*. *$P \leq 0.05$ (Student *t* test). *F*: Fasting HOMA-IR from *ob/ob* mice injected intraperitoneally with curcusomes for 4 weeks. ***$P \leq 0.001$ (one-way ANOVA followed by Bonferroni post hoc test).

mice. Transfer of hepatic Tip-DCs or ATMs impaired GTT in NOB recipients. In contrast, the same cells isolated from curcusome-treated *ob/ob* mice showed no impairment of GTT (Fig. 6*D*). These results indicate that both hepatic Tip-DCs and ATMs promote insulin resistance and that suppression of either hepatic Tip-DC or ATM function with curcusomes is sufficient to prevent insulin resistance in obese mice.

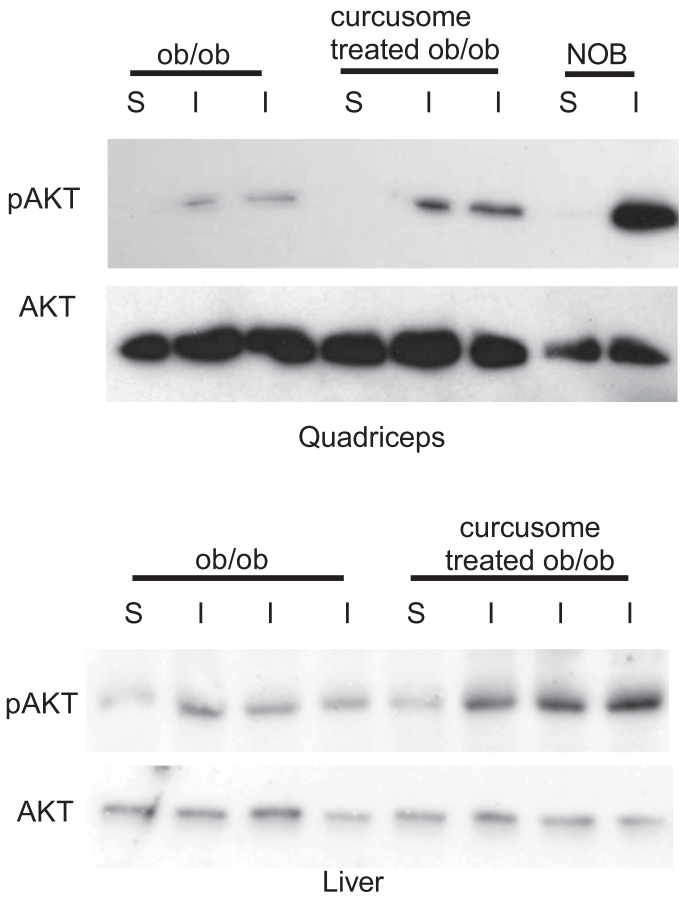

FIG. 5. Improved insulin signaling in tissues isolated from *ob/ob* mice treated with curcusomes. Lysates of quadriceps and liver from curcusome-treated or untreated *ob/ob* mice signaled with (I) or without (S) insulin were analyzed by SDS-PAGE and immunoblotted for pAKT (ser473) and AKT. Induction of pAKT in NOB mice after insulin injection was used as a positive control for the experiment.

DISCUSSION

The majority of obesity-related problems, such as type 2 diabetes, have been shown to stem from a low-grade proinflammatory state (14). Increased activation of proinflammatory signaling pathways such as NF-κB and an associated increase in production of proinflammatory molecules from macrophages have been implicated in obesity-related pathophysiological states (15). ATMs are of particular interest because they accumulate with weight gain and produce TNF and IL-6, which promote insulin resistance (16). ATMs are heterogeneous, including both CD11c+ and CD11c− phenotypes. However, the CD11b+F4/80+CD11c+ population is increased in obesity and has a proinflammatory phenotype (1). Moreover, in *ob/ob* mice reconstituted with bone marrow from CD11c-diphtheria toxin receptor transgenic mice, ablation of CD11c+ ATMs with diphtheria toxin prevents insulin resistance (17). These findings indicate that targeting CD11c+ ATMs is likely to be beneficial in treating type 2 diabetes. In addition to ATMs, hepatic macrophages also contribute to insulin resistance by release of systemic inflammatory mediators, as shown by studies where depletion of Kuppfer cells using liposomes containing chlodronate prevented the development of insulin resistance (18).

Obese mice fed a high-fat diet were able to normalize skeletal muscle and adipose tissue insulin sensitivity, but not hepatic insulin sensitivity, after dietary normalization, indicating a dissociation of hepatic steatosis from insulin resistance (3). It is intriguing that this reversal does not seem to correlate with a reduction of CD11c+ ATM numbers but rather, a reversal of their proinflammatory state, indicating that ATMs have the potential to be inhibited in response to appropriate cell signals or tissue factors (3). These studies indicate that even with dietary intervention, it may also be essential to target hepatic inflammatory macrophages for treatment of insulin resistance.

The polyphenol curcumin is considered the most active component in *Curcuma longa* (or turmeric), a popular dietary spice used in Southeast Asian countries (19). Curcumin inhibits the activation of NF-κB and TLR-4 proinflammatory signaling pathways in mouse models and does so without any dose-limiting toxicities (20–23). Moreover, curcumin supplementation by gavage in SD rats injected with streptozotocin reversed diabetic markers, such as blood levels of IL-6, MCP-1, TNF, glucose, glycosylated hemoglobin, and oxidative stress (24), indicating that curcumin supplementation can reduce hyperglycemia and the risk of vascular inflammation in diabetes. However, the bioavailability of oral curcumin is low, and other modes of delivery will be required to exploit its therapeutic properties (7). Liposomes, wherein curcumin is encapsulated in a lipid bilayer, have been shown to be an effective curcumin delivery method in different disease settings in vivo (8). In this study, *ob/ob* mice were used to explore whether curcusomes could be delivered to inflammatory macrophages and whether this inhibited NF-κB signaling and proinflammatory cytokine production. Curcusomes inhibited the zymosan-induced oxidative burst, in peritoneal macrophages, and NF-κB–induced IL-6 production by liver Tip-DCs and ATMs isolated from *ob/ob* mice, and both these populations were able to transfer insulin resistance to NOB mice unless inhibited by curcusomes. Thus, encapsulation into liposomes overcomes the bioavailability problems of curcumin and effectively targets curcumin to the phagocytic inflammatory antigen-presenting cells that mediate insulin resistance in obese mice.

It is surprising that we identified a population of TNF- and iNOS-expressing DCs in the liver of *ob/ob* mice. These macrophages share similarities to recently described inflammatory liver DCs or Tip-DCs that play an important role in pathogen clearance. Tip-DCs develop from bone marrow–derived CD11b+Ly6C+ inflammatory monocytes, which differentiate into CD11c+ and CD80/CD86/MHC-II low immature inflammatory DCs in the liver, by a CCR2-dependent process (13). In response to pathogen and IFN-γ, Tip-DCs can differentiate to TNF+, iNOS+, and CD80/CD86/MHC-II high mature inflammatory DCs that lead to liver damage that is preventable with IL-10 (13). The increase of this population in *ob/ob* mice and their proximity to fat-laden hepatocytes suggest that activated hepatocytes in the steatotic liver secrete chemokines that induce recruitment and development of Tip-DCs, in synergy with alternate TLR-4 damage–associated ligands, such as free fatty acids, and with T-cell–derived IFN-γ. Since hepatic Tip-DCs could be further activated to express increased amounts of TNF and iNOS by ex vivo culture, they may not be fully activated in the obese environment. This is significant, in light of the sensitivity of *ob/ob* mice to endotoxin-associated liver damage, which might also be preventable with curcusomes (25). Tip-DCs may also be relevant to human liver disease, where 15% of all patients with non–alcohol-related fatty liver disease and associated steatosis develop steatohepatitis, characterized by hepatocellular injury, inflammation, and fibrosis (26). These patients

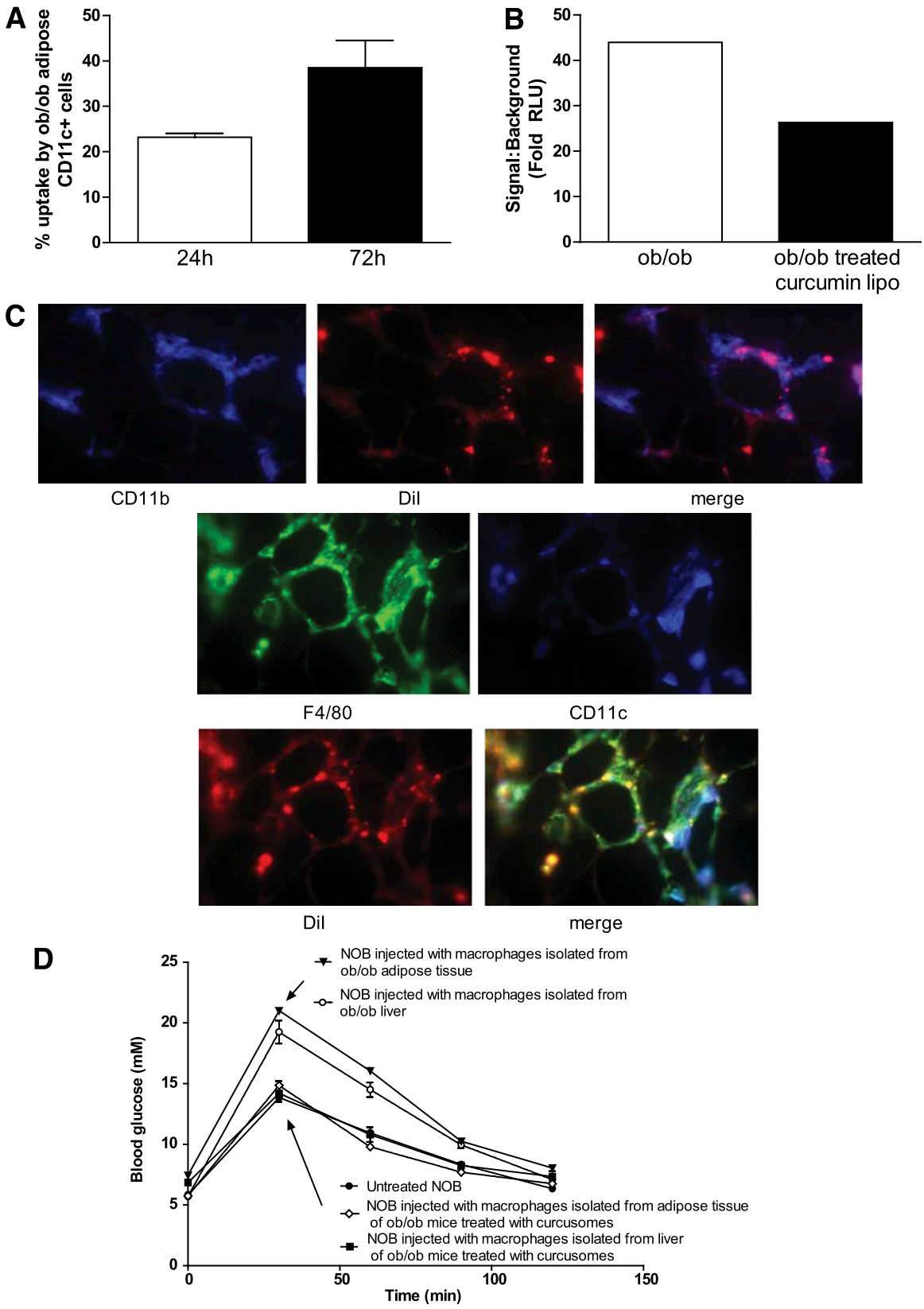

FIG. 6. In vivo delivery of curcusomes inhibits adipose tissue inflammatory DC nuclear RelA and promotes insulin sensitivity. *A*: *Ob/ob* mice were injected intraperitoneally with DiI-curcusomes, and gradient-purified cells were harvested at 24 and 72 h and stained for MHC class II and CD11c. Shown are the percentages of CD11c+ cells that are DiI+. Data are mean ± SEM of two separate experiments. *B*: Nuclear extracts from CD11c+ ATM isolated from *ob/ob* mice injected with or without curcusomes for 24 h were analyzed for DNA binding of RelA by chemiluminescence. Shown is the mean of duplicates from two separate experiments. *C*: *Ob/ob* mice were injected intraperitoneally with DiI-curcusomes for 72 h and then adipose tissue was harvested, frozen in optimal cutting temperature media, sectioned, and stained with CD11b (blue) or F4/80 (green) and CD11c (blue) antibodies. DiI staining is indicated in red; images analyzed by immunofluorescence microscopy. Original magnification ×25. *D*: GTT from NOB mice injected intravenously with 1×10^6 F4/80+ DCs from adipose tissue or liver tissue from *ob/ob* mice treated with or empty liposomes or curcusomes for 24 h. (A high-quality digital representation of this figure is available in the online issue.)

develop liver cirrhosis and hepatocellular carcinoma at increased rates.

Inhibition of Tip-DC–dependent inflammation may occur through a number of mechanisms. In this study, we show that curcusomes are taken up by Tip-DCs after intraperitoneal injection and that Tip-DCs show impaired induction of nuclear RelA, reduced production of TNF and IL-6, and increased IL-4. This correlated with improvements in insulin resistance, both in the short-term and over a longer 4-week experiment. It is important that IL-4 has been shown to induce an alternative activated signature in liver macrophages in a peroxisome proliferator–activated receptor-δ dependent process. On the other hand, ATMs require peroxisome proliferator–activated receptor-γ for alternate activation (27,28). Thus, curcusomes may not only reduce macrophage inflammation through direct effects on NF-κB but also further induce alternate macrophage pathways indirectly, through IL-4.

In this study, curcusome therapy had minimal impact on proportions of Tip-DCs and other leukocytes within the liver, indicating that the insulin-sensitizing effects of curcusomes were not due to death or alterations in recruitment of inflammatory cells to the liver, at least during the 72 h after treatment. Moreover, a single dose of curcusomes imparted longer term improvements in insulin signaling for at least 4 weeks. The longer term benefits are likely to relate to specific targeting and/or the long-lived properties of macrophages. Curcusomes targeted hepatic macrophages, which improved insulin signaling as measured by insulin-induced pAKT in the liver. Insulin signaling was also improved in the muscle, indicating improvements in systemic insulin resistance.

Liver sensitivity to obesity and endotoxin may also be regulated by numbers of and cytokine production by NKT cells or regulatory T cells in the liver. NKT cells recognize CD1d, which is expressed by CD11c+ DCs (29,30). NKT cells may secrete cytokines such as IL-10 and IL-4 that could suppress Tip-DC function (31,32). In this regard, *ob/ob* mice have reduced numbers of NKT cells in the liver, and transfer of NKT cells has been shown to improve insulin sensitivity (33,34). The mechanism behind improvements is likely through suppression of hepatic Tip-DC and ATM activation. Although we also observed reduced numbers of NKT cells in the livers of *ob/ob* mice, curcusome injection did not increase numbers of hepatic NKT cells. However, we cannot rule out the possibility that lipid components in combination with curcumin may promote cytokines from existing NKT cells that suppress Tip-DCs. Adipose tissue regulatory T cells may also provide a source of IL-10, since obesity correlates with a reduction in regulatory T cells in visceral adipose tissue and expansion of regulatory T-cell number with oral anti-CD3, or by adoptive transfer prevents onset of insulin resistance (35,36). Further work is needed to determine whether curcusomes suppress inflammation-induced insulin resistance through these regulatory networks, particularly in light of our previous work demonstrating that curcusomes inhibit inflammatory arthritis through induction of regulatory T cells. In conclusion, curcusome nanoparticles inhibit proinflammatory pathways in hepatic Tip-DCs and ATMs and reverse insulin resistance. Targeting inflammatory DCs is a promising approach for type 2 diabetes prevention and treatment.

ACKNOWLEDGMENTS

This work was supported by National Health and Medical Research Council grants 351439 and 569938. R.T. has received support from Arthritis Queensland and an Australian Research Council Future Fellowship. B.O. has received support from a Queensland Government Smart State Fellowship sponsored by Arthritis Queensland.

No potential conflicts of interest relevant to this article were reported.

S.K.Y. researched data. R.T. wrote the manuscript. B.O. researched data and wrote the manuscript.

REFERENCES

1. Nguyen MT, Favelyukis S, Nguyen AK, et al. A subpopulation of macrophages infiltrates hypertrophic adipose tissue and is activated by free fatty acids via toll-like receptors 2 and 4 and JNK-dependent pathways. J Biol Chem 2007;282:35279–35292
2. Arkan MC, Hevener AL, Greten FR, et al. IKK-beta links inflammation to obesity-induced insulin resistance. Nat Med 2005;11:191–198
3. Li P, Lu M, Nguyen MT, et al. Functional heterogeneity of CD11c-positive adipose tissue macrophages in diet-induced obese mice. J Biol Chem 2010; 285:15333–15345
4. Hevener AL, Olefsky JM, Reichart D, et al. Macrophage PPAR gamma is required for normal skeletal muscle and hepatic insulin sensitivity and full antidiabetic effects of thiazolidinediones. J Clin Invest 2007;117:1658–1669
5. Shah P, Mudaliar S. Pioglitazone: side effect and safety profile. Expert Opin Drug Saf 2010;9:347–354
6. Weisberg SP, Leibel R, Tortoriello DV. Dietary curcumin significantly improves obesity-associated inflammation and diabetes in mouse models of diabesity. Endocrinology 2008;149:3549–3558
7. Sharma RA, Steward WP, Gescher AJ. Pharmacokinetics and pharmacodynamics of curcumin. Adv Exp Med Biol 2007;595:453–470
8. Marczylo TH, Verschoyle RD, Cooke DN, Morazzoni P, Steward WP, Gescher AJ. Comparison of systemic availability of curcumin with that of curcumin formulated with phosphatidylcholine. Cancer Chemother Pharmacol 2007;60:171–177
9. Chen C, Johnston TD, Jeon H, et al. An in vitro study of liposomal curcumin: stability, toxicity and biological activity in human lymphocytes and Epstein-Barr virus-transformed human B-cells. Int J Pharm 2009;366: 133–139
10. Capini C, Jaturanpinyo M, Chang HI, et al. Antigen-specific suppression of inflammatory arthritis using liposomes. J Immunol 2009;182:3556–3565
11. Müller-Peddinghaus R. In vitro determination of phagocyte activity by luminol- and lucigenin-amplified chemiluminescence. Int J Immunopharmacol 1984; 6:455–466
12. Bhattacharya N, Sarno A, Idler IS, et al. High-throughput detection of nuclear factor-kappaB activity using a sensitive oligo-based chemiluminescent enzyme-linked immunosorbent assay. Int J Cancer 2010;127: 404–411
13. Bosschaerts T, Guilliams M, Stijlemans B, et al. Tip-DC development during parasitic infection is regulated by IL-10 and requires CCL2/CCR2, IFN-gamma and MyD88 signaling. PLoS Pathog 2010;6:e1001045
14. Must A, Spadano J, Coakley EH, Field AE, Colditz G, Dietz WH. The disease burden associated with overweight and obesity. JAMA 1999;282:1523–1529
15. Hassan MK, Joshi AV, Madhavan SS, Amonkar MM. Obesity and health-related quality of life: a cross-sectional analysis of the US population. Int J Obes Relat Metab Disord 2003;27:1227–1232
16. Weisberg SP, McCann D, Desai M, Rosenbaum M, Leibel RL, Ferrante AW Jr. Obesity is associated with macrophage accumulation in adipose tissue. J Clin Invest 2003;112:1796–1808
17. Patsouris D, Li PP, Thapar D, Chapman J, Olefsky JM, Neels JG. Ablation of CD11c-positive cells normalizes insulin sensitivity in obese insulin resistant animals. Cell Metab 2008;8:301–309
18. Wunderlich FT, Ströhle P, Könner AC, et al. Interleukin-6 signaling in liver-parenchymal cells suppresses hepatic inflammation and improves systemic insulin action. Cell Metab 2010;12:237–249
19. Hatcher H, Planalp R, Cho J, Torti FM, Torti SV. Curcumin: from ancient medicine to current clinical trials. Cell Mol Life Sci 2008;65:1631–1652
20. Lao CD, Ruffin MT 4th, Normolle D, et al. Dose escalation of a curcuminoid formulation. BMC Complement Altern Med 2006;6:10
21. Bharti AC, Takada Y, Aggarwal BB. Curcumin (diferuloylmethane) inhibits receptor activator of NF-kappa B ligand-induced NF-kappa B activation in osteoclast precursors and suppresses osteoclastogenesis. J Immunol 2004; 172:5940–5947

22. Kunnumakkara AB, Guha S, Krishnan S, Diagaradjane P, Gelovani J, Aggarwal BB. Curcumin potentiates antitumor activity of gemcitabine in an orthotopic model of pancreatic cancer through suppression of proliferation, angiogenesis, and inhibition of nuclear factor-kappaB-regulated gene products. Cancer Res 2007;67:3853–3861
23. Shakibaei M, John T, Schulze-Tanzil G, Lehmann I, Mobasheri A. Suppression of NF-kappaB activation by curcumin leads to inhibition of expression of cyclo-oxygenase-2 and matrix metalloproteinase-9 in human articular chondrocytes: implications for the treatment of osteoarthritis. Biochem Pharmacol 2007;73:1434–1445
24. Jain SK, Rains J, Croad J, Larson B, Jones K. Curcumin supplementation lowers TNF-alpha, IL-6, IL-8, and MCP-1 secretion in high glucose-treated cultured monocytes and blood levels of TNF-alpha, IL-6, MCP-1, glucose, and glycosylated hemoglobin in diabetic rats. Antioxid Redox Signal 2009; 11:241–249
25. Yang SQ, Lin HZ, Lane MD, Clemens M, Diehl AM. Obesity increases sensitivity to endotoxin liver injury: implications for the pathogenesis of steatohepatitis. Proc Natl Acad Sci USA 1997;94:2557–2562
26. Marrero JA, Fontana RJ, Su GL, Conjeevaram HS, Emick DM, Lok AS. NAFLD may be a common underlying liver disease in patients with hepatocellular carcinoma in the United States. Hepatology 2002;36:1349–1354
27. Odegaard JI, Ricardo-Gonzalez RR, Goforth MH, et al. Macrophage-specific PPARgamma controls alternative activation and improves insulin resistance. Nature 2007;447:1116–1120
28. Odegaard JI, Ricardo-Gonzalez RR, Red Eagle A, et al. Alternative M2 activation of Kupffer cells by PPARdelta ameliorates obesity-induced insulin resistance. Cell Metab 2008;7:496–507
29. Swain MG. Natural killer T cells within the liver: conductors of the hepatic immune orchestra. Dig Dis 2010;28:7–13
30. Godfrey DI, Kronenberg M. Going both ways: immune regulation via CD1d-dependent NKT cells. J Clin Invest 2004;114:1379–1388
31. Nowak M, Stein-Streilein J. Invariant NKT cells and tolerance. Int Rev Immunol 2007;26:95–119
32. La Cava A, Van Kaer L, Fu-Dong-Shi. CD4+CD25+ Tregs and NKT cells: regulators regulating regulators. Trends Immunol 2006;27:322–327
33. Guebre-Xabier M, Yang S, Lin HZ, Schwenk R, Krzych U, Diehl AM. Altered hepatic lymphocyte subpopulations in obesity-related murine fatty livers: potential mechanism for sensitization to liver damage. Hepatology 2000;31: 633–640
34. Elinav E, Pappo O, Sklair-Levy M, et al. Adoptive transfer of regulatory NKT lymphocytes ameliorates non-alcoholic steatohepatitis and glucose intolerance in ob/ob mice and is associated with intrahepatic CD8 trapping. J Pathol 2006;209:121–128
35. Feuerer M, Herrero L, Cipolletta D, et al. Lean, but not obese, fat is enriched for a unique population of regulatory T cells that affect metabolic parameters. Nat Med 2009;15:930–939
36. Ilan Y, Maron R, Tukpah AM, et al. Induction of regulatory T cells decreases adipose inflammation and alleviates insulin resistance in ob/ob mice. Proc Natl Acad Sci USA 2010;107:9765–9770